



## **Structural Studies on Citrate Capped Gold Nanoparticles Dispersed in Liquid Crystals**

M.Tejaswi<sup>1</sup>, G.Giridhar<sup>2</sup>, M.C. Rao<sup>3</sup> and RKNR Manepalli<sup>1\*</sup>

<sup>1</sup>Department of Physics, The Hindu College, Krishna University, Machilipatnam-521001, India

<sup>2</sup>Department of Nanotechnology, Acharya Nagarjuna University, Guntur-522510, India

<sup>3</sup>Department of Physics, Andhra Loyola College, Vijayawada-520008, India

**Abstract** : Liquid crystals act as tunable solvents for the dispersion of nanomaterials and they are being anisotropic media, provide a very good support for the self assembly of nanomaterials in to large organized structures in multiple dimensions. Nanoobjects that are dispersed in the liquid crystals can trap ions, which decrease the ion concentration and electrical conductivity and improve the electro-optical response of the host. The synthesis and characterization are carried out on liquid crystalline *p*-decyloxy benzoic acid *p*-undecyloxy benzoic acid (10OBA & 11OBA) with 30 $\mu$ l citrate capped Gold (Au) nanoparticles dispersion. Spectroscopic techniques like XRD, SEM, FTIR and DSC were performed on to the prepared samples. The results showed that the dispersion of citrate capped Au nanoparticles in 10OBA and 11OBA exhibited nematic phases as same as the pure liquid crystals, with reduced clearing temperature as expected. The smectic-C thermal ranges are enhanced and the nematic thermal ranges are changed slightly in DSC with the dispersion of citrate capped Au nanoparticles.

**Keywords** : Synthesis, Polarizing Optical Microscope (POM), Differential Scanning Calorimeter (DSC), Nano dispersion, X-ray Diffraction studies (XRD), Scanning Electron Microscopy (SEM) and Fourier Transform Infra Red Spectroscopy (FTIR).

### **Introduction:**

Liquid crystals (LCs) are mesophases with a degree of order in between that of solid and liquid exhibiting anisotropic properties. LCs are self assembled dynamic functional soft materials which possess both order and mobility at molecular, supra molecular and microscopic levels<sup>1-3</sup>. The anisotropy properties include birefringence, viscosity, elasticity, dielectric permittivity, etc. The flow property allows them to be contained in any container. These two properties make these LC materials as viable candidates for applications. Recently, nanomaterials are used in one of the most fruitful factors in new approaches to the nonlinear optics field. Additionally, liquid crystals are very welcoming to other materials which are mixed with nanoparticles or embedded into other materials/confinements very well. This creates an opportunity for the construction of a whole new world of composite materials such as liquid crystalline nanomaterials.

More over, metal nano clusters, particularly gold nanoparticles, have attracted a great deal of interest since they show unusual properties compared to bulk metals. Gold nanoparticles are the most stable metal nanoparticles and they present fascinating aspects such as, their self-assembly, the behaviour of individual particles, size related electronic, magnetic and optical properties and their applications as catalysis<sup>4</sup>. They also find applications in biological sciences<sup>5</sup>. The synthesis of monolayer-protected gold nanoparticles in organic solvents by Brust et al.<sup>6</sup> have opened new field in material science. Since the properties of metal nanocluster

aggregates are affected by their morphology, various attempts to control their morphology have been performed by means of physical<sup>7</sup> and chemical processes<sup>8</sup>. Rao et al. have presented the results on different oxide materials in their earlier studies<sup>9-14</sup>.

In the present paper citrate capped Au nanoparticles dispersed in liquid crystalline compounds *p*-decyloxy benzoic acid and *p*-undecyloxy benzoic acid were synthesized and characterized by DSC, SEM, XRD and birefringence.

## Experimental:

### Synthesis of Citrate capped Au nanoparticles:

LC compounds 10OBA & 11OBA, Auric Chloride (HAuCl<sub>4</sub>) and trisodium citrate dehydrate (Na<sub>3</sub>C<sub>6</sub>H<sub>5</sub>O<sub>7</sub>•2H<sub>2</sub>O) 99% are brought from Sigma-Aldrich laboratories, USA and used as such. Citrate capped Au nanoparticles are synthesized in the laboratory from the citrate reduction process. First, 20ml of 1mM of Auric Chloride is heated and 2ml of 1% trisodium citrate is added drop by drop and stirred vigorously for two hours. Then the solution changed gradually to red wine color indicates the formation of citrate capped Au nanoparticles. The citrate capped Au nanoparticles synthesized by this manner as citrate served the dual purpose of being the reducing agent as well as stabilizer.

### Dispersion of nanoparticles into the LC compounds:

For uniform dispersion of nanoparticles in LCs, the nanoparticles are first dissolved in ethyl alcohol, stirred well about 45 minutes and later introduced in the isotropic state of mesogenic material (10OBA & 11OBA) in quantity 30μl and 50μl separately. After cooling, the nanocomposite 10OBA & 11OBA is subjected to study of the textural and phase transition temperatures using a polarizing optical microscope (SDTECHS make) with a hot stage in which the substance was filled in planar arrangement in 4 μm cells and these could be placed along with the thermometer described by Gray<sup>15</sup>. Textural and phase transition temperatures are studied after preparation of the sample and observations are made again to understand the stability of nanoparticles. The presence of citrate capped Au nanoparticles in 10OBA & 11OBA is studied by UV and SEM data and existence as well as size is determined by XRD technique.

## Results and Discussion:

### Polarizing Optical Microscope:

The liquid crystalline molecule is characterized by different Liquid Crystalline phases due to the change in the local molecular order with the temperature giving rise to different phases. Determination and characterization of these mesophases will provide very important information on the pattern and textures of the liquid crystals. The transition temperatures and textures observed by Polarizing Microscope in 10OBA pure are shown in Fig.1(a-c) while that of with dispersed citrate capped Au nanoparticles with concentration 30μl shown in Fig.2(a-c) respectively. The thermal ranges of nematic phase are changed slightly due to the dispersion of nanoparticles and the textures of the phase's changes by the self assembly of nanoparticles. The DSC thermograms are shown in Fig.3 to Fig.6. The transition temperatures at the phase transformations determined through POM is shown in the Table-1. It is observed that the transition temperatures are lowered slightly with the dispersion of citrate capped Au nanoparticles dispersed in 10OBA and 11OBA.

**10OBA Pure**

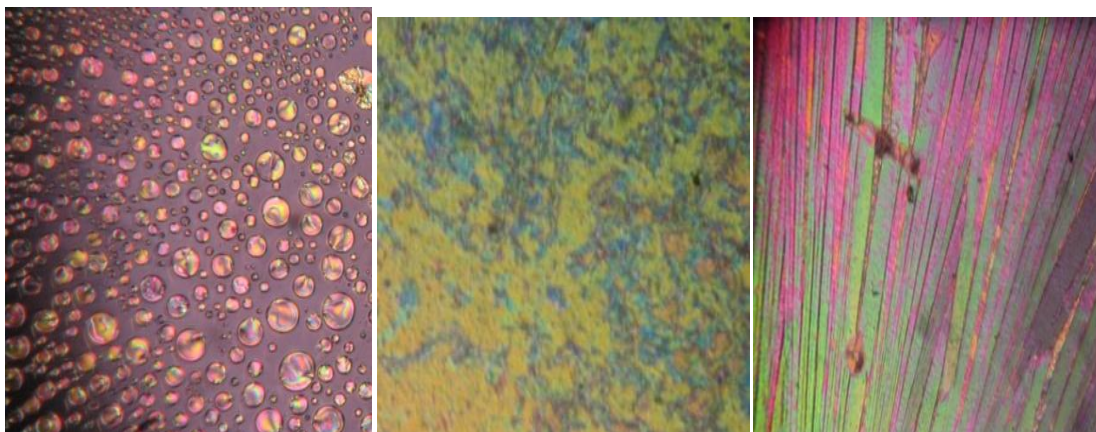


**Fig.1a**Nematic phase **Fig.1b**Smectic C phase**Fig.1c**Solid phase at138.7°C at 119.9°Cat 91.5°C

**10OBA + 30 $\mu$ lct capped Au**

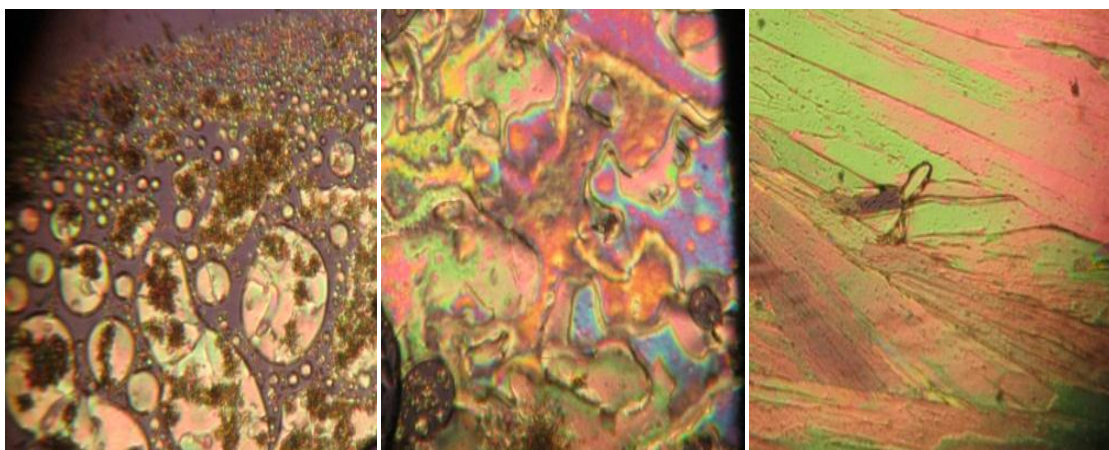


**Fig.2a** Nematic phase **Fig.2b** Smectic C phase**Fig. 2c** Solidphase at137.7°C at 118.5°Cat 71.5°C

**DSC Thermograms**

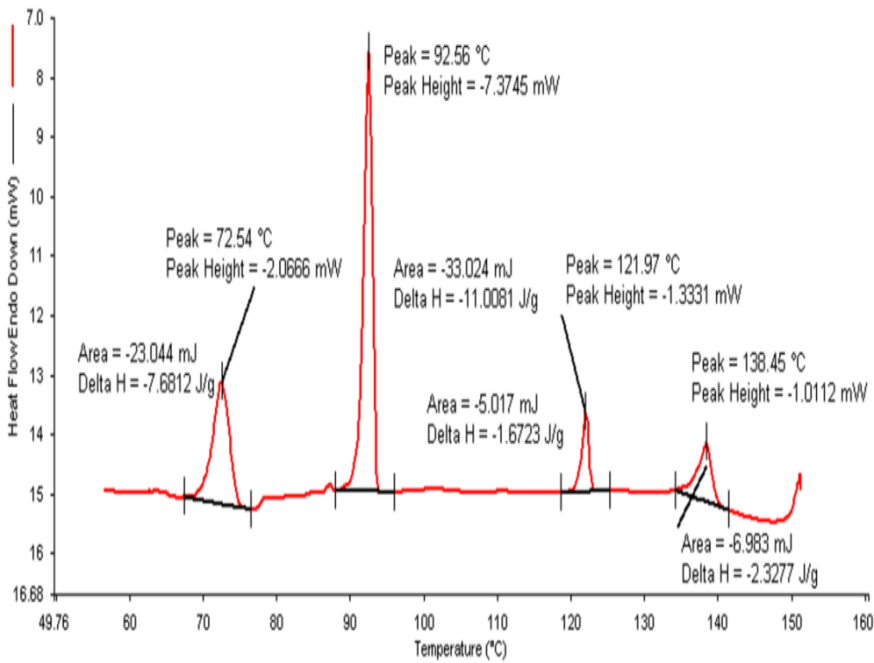


**Fig.3 DSC Thermogram of 10OBA Pure**

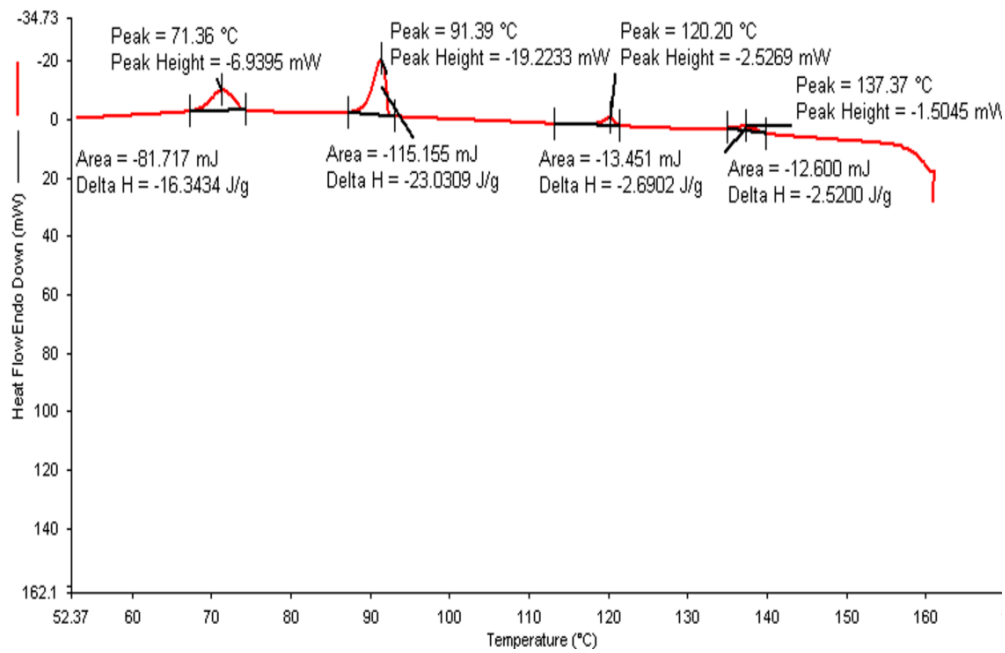


**Fig.4 DSC Thermogram of 10OBA Pure + 30µl ct capped Au nanoparticles**

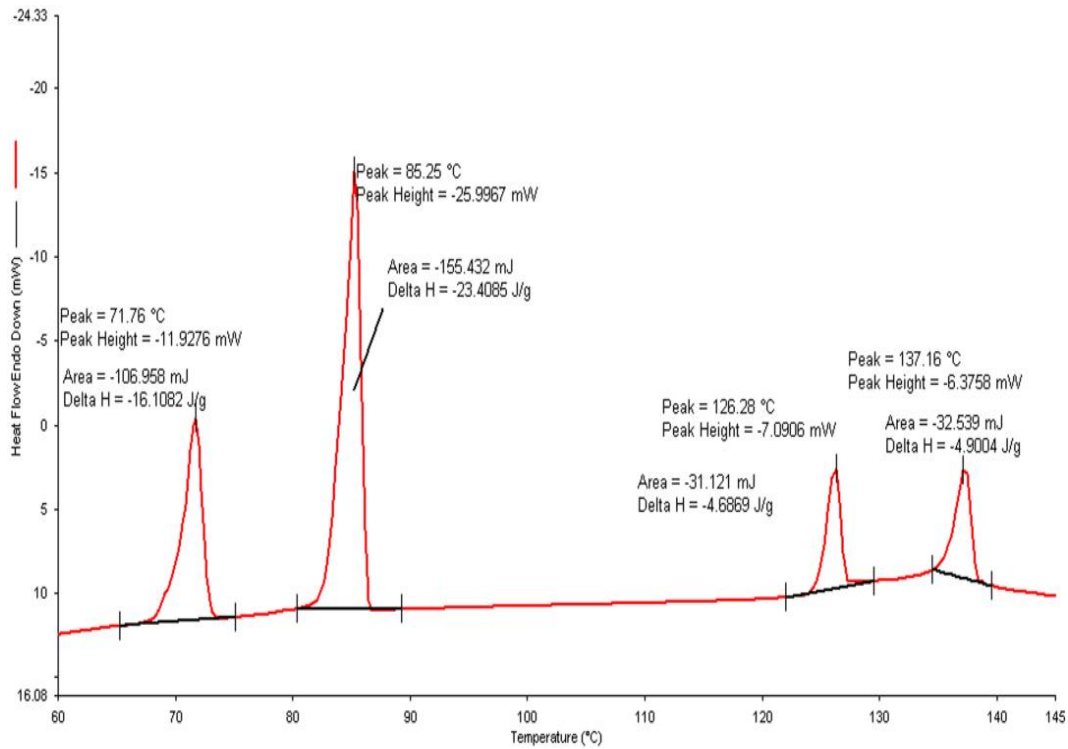


**Fig.5**DSC Thermogram of 11OBA Pure

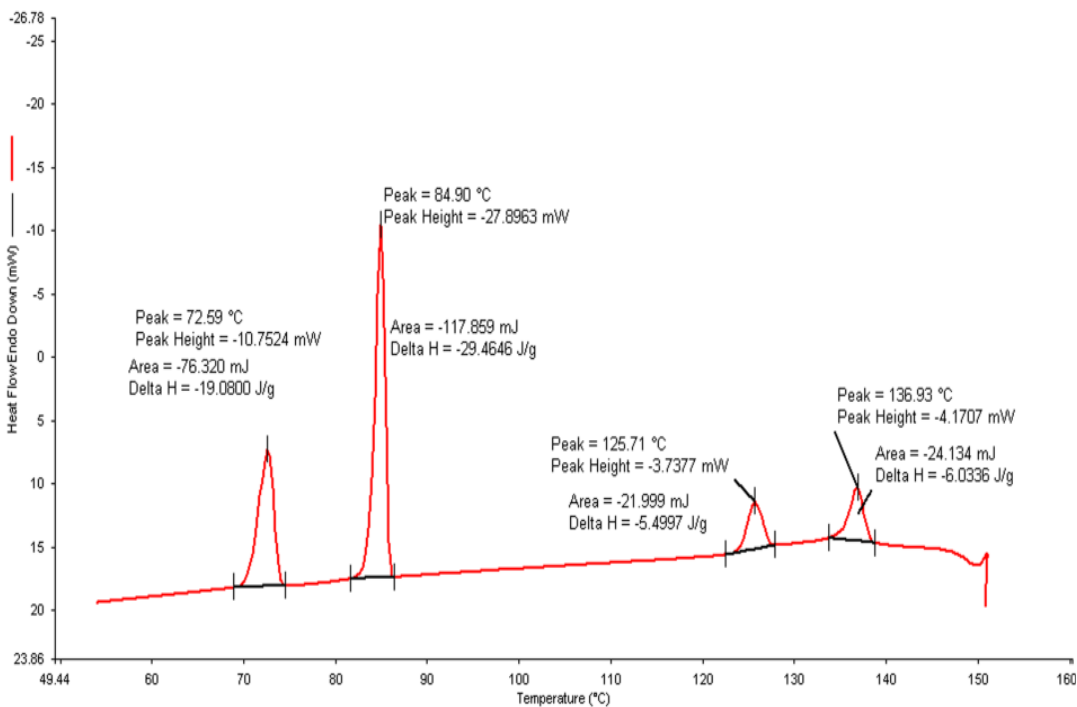


**Fig.6**DSC Thermogram of 11OBA Pure + 50µl ct capped Au nanoparticles

**Table-1**Phase variants, transition temperatures, Enthalpy values of 10OBA and 11OBA pure and with dispersed 30  $\mu$ l and 50 $\mu$ l citrate capped Aunanoparticles

S. No	Compound	DSC/ POM	Scan Rate	Transition Temperatures °C				Thermal Ranges	
				I-N	N-SmC	SmC-SolidI	Solid I – Solid II	$\Delta n$	$\Delta SmC$
1	10OBA PURE	DSC	20c/m in $\Delta HJ/g$	138.45 2.327	121.97 1.6723	92.56 11.01	72.54 7.68	16.48	29.41
		POM		138.9	122.8	91.5	70.2	16.1	31.3
2	10OBA +30 $\mu$ l ct capped Au	DSC	20c/m in $\Delta HJ/g$	138.09 2.520	119.35 2.6902	90.47 23.03	73.13 16.34	18.74	28.88
		POM		137.7	118.5	91.5	70.3	19.2	27
3	11OBA PURE	DSC	20c/m in $\Delta HJ/g$	137.1 4.900	126.3 4.6809	85.2 23.41	71.8 16.11	10.8	41.1
		POM		137.4	126.3	86	71.2	11.1	40.3
4	11OBA +50 $\mu$ l ct capped Au	DSC	20c/m in $\Delta HJ/g$	136.93 6.033	125.71 5.499	84.9 29.46	72.59 19.08	11.22	40.81
		POM		136.2	124.4	83.2	73.9	11.8	41.2

**Ultraviolet –Visible Spectroscopy:**

The Fig.7 shows the UV-visible spectra of 10OBA pure, pure citrate capped Au nanoparticles and citrate capped Au nanoparticles dispersed in 10OBA LC sample. It is observed that the spectrum for pure 10OBA does not exhibit any absorption peaks in the wavelength range of 500–600nm. However, the spectrum of nanodoped 10OBA shows the significant peak at 550nm, which is the characteristic peak of citrate capped Au nanoparticles. The decrease of absorbance peak in 10OBA with the dispersion of citrate capped Ag nanoparticles resembles the capping of nanoparticles with 10OBA. So, the UV-visible spectral study confirms the presence of citrate capped Ag nanoparticles in 10OBA.

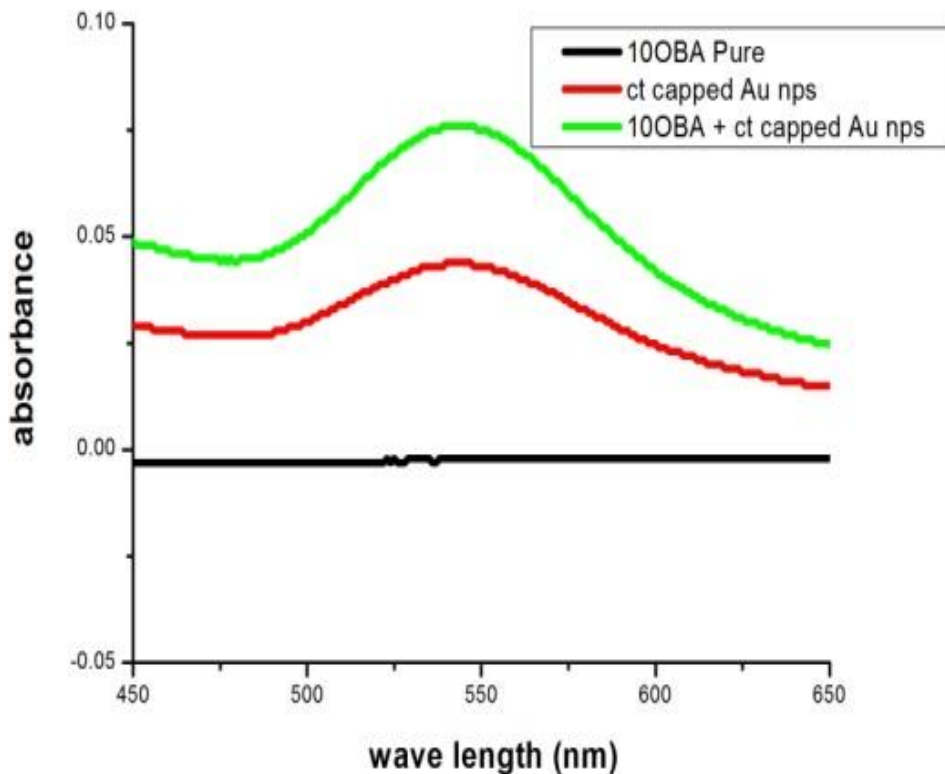
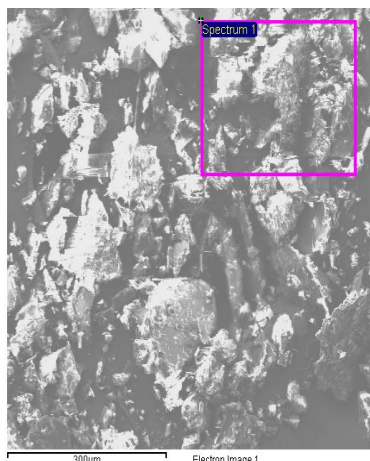
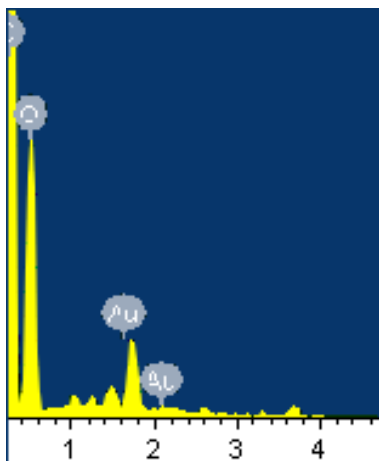


**Fig. 7** UV-visible spectra of 10OBA with dispersed 50µl citrate capped Au nanoparticles

**SEM analysis:** SEM gives the magnified image of the surface of a material, topographical information and also gives the information regarding the composition of the elements in the material. The SEM image and EDS data of 10OBA with the dispersion of 50µl of ct capped Au nanoparticles in 10OBA is shown in the Fig. 8 and Fig.9.



Element	Weight%	Atomic%
C K	66.75	73.42
O K	32.09	26.50
Au M	1.17	0.08

**Fig 8** EDS data of 10OBA + 50µl citrate capped Au Nanoparticles

**Fig.9** SEM Image of 10OBA + citrate capped Au Nanoparticles 50µl

**XRD Analysis:**The XRD data of 10OBA with dispersed 50 $\mu$ l ct capped Au nanoparticles are shown in Fig. 10.

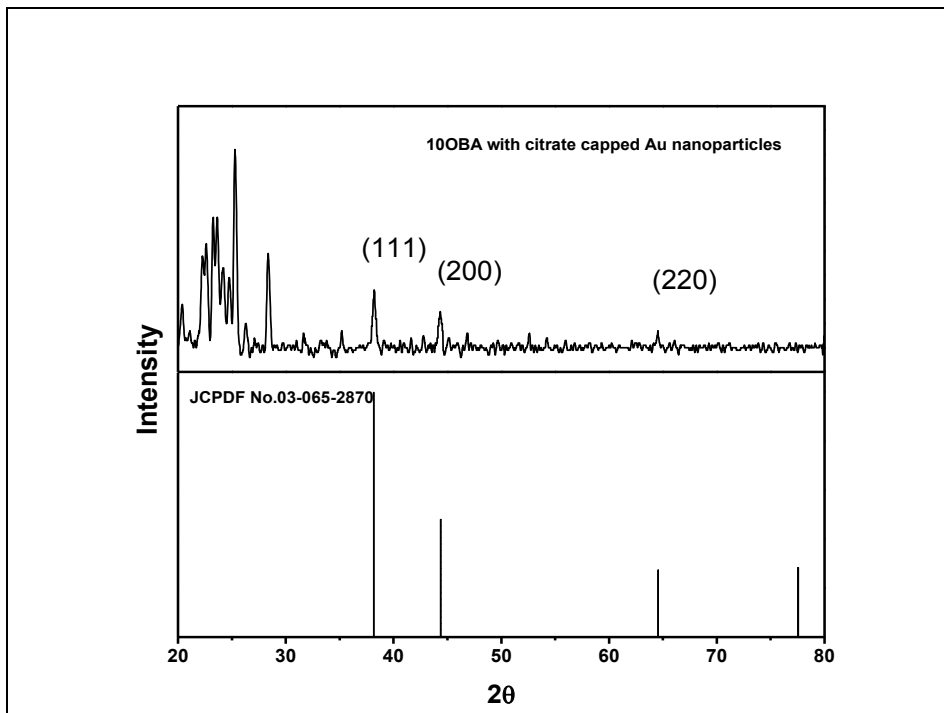


**Fig.10**XRD of 10OBA with 50 $\mu$ l of ct capped Au nanoparticles

In comparison of JCPDF data peaks were well resolved and are matched with JCPDF card no.03-065-2870 which is clearly evidenced the existence of ct capped Au nanoparticles. By using Scherrer's Formula,  $t = k\lambda / \beta \cos\theta$ , grain size 29 nm,  $\Lambda = 1.54 \text{ \AA}$ ,  $\beta = \text{FWHM}$ , Peaks at  $38.39^\circ$ ,  $44.24^\circ$  and  $64.55^\circ$  resembles the existence of ct capped Au nanoparticles.

### Estimation of Orientational Order parameter S from Refractive Indices Data:

#### (a) Optical Birefringence Studies:

The Modified spectrometer is used to determine the refractive indices of 10OBA pure and 10OBA with 50 $\mu$ l ct capped Au nanoparticles dispersion are measured. A wedge shaped cell with temperature accuracy  $\pm 0.1^\circ\text{C}$  is used to determine the refractive indices  $n_e$  and  $n_o$  at wavelength 589.3 nm. The refractive index in the isotropic phase shows very nominal increment with the decrease of the temperature. The rotational symmetry of molecules in liquid crystals is broken at the I-N phase transition, and thereby the isotropic value splits into two, one value higher and another lower than isotropic value corresponding to extraordinary ( $n_e$ ) and ordinary ( $n_o$ ) refractive indices respectively. Fig. 11 and Fig.12 represent the variation of refractive indices in 10OBA and 10OBA with 50 $\mu$ l ct capped Au nanoparticles. It is found that I-N transition temperature decreased with nanoparticles dispersion which is shown in the DSC and POM values. Further, the birefringence values obtained for 10OBA is nearly equal with the previously published data<sup>16</sup>. Birefringence property and its dependency on molecular reorientation play an important role in understanding the molecular reorientation mechanisms<sup>17,18</sup>. It is further found that the birefringence anisotropy,  $\delta n = n_e - n_o$  values with respect to temperature increases with the dispersion of ct capped Au nanoparticles as shown in the Fig.13. It resembles the self alignment of nanoparticles with 10OBA molecules with the Au nanoparticles and thereby the view angle increases which will be very much useful display devices.

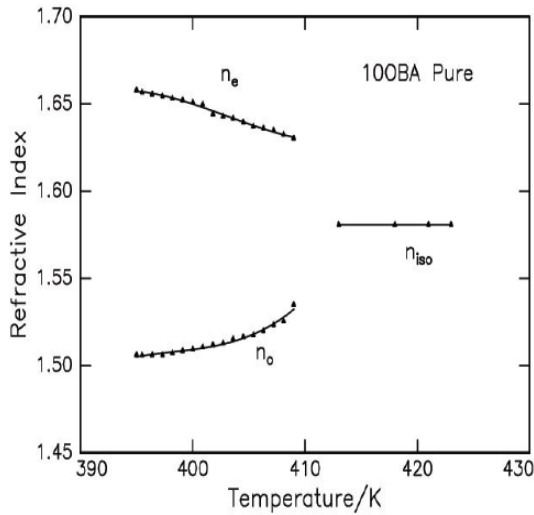


**Fig.11**Refractive index of 100BA pure

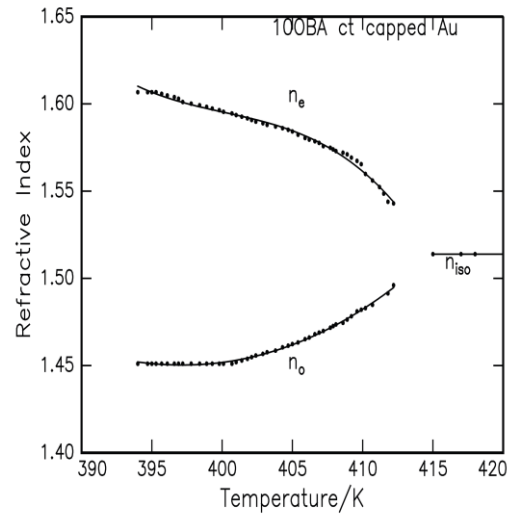


**Fig.12**Refractive index of 100BA + 50µl ct capped Au

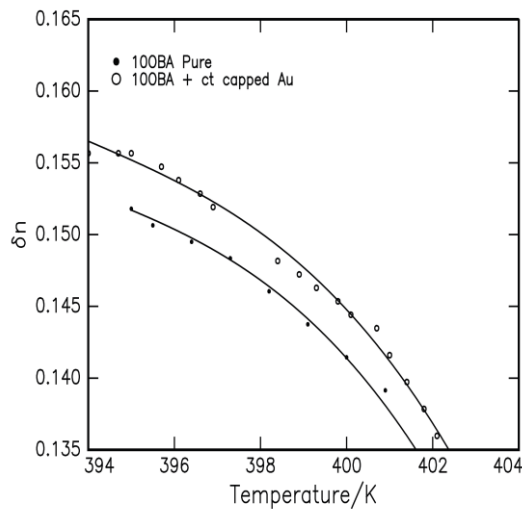


**Fig.13** Variation of  $\delta n$  with temperature in 100BA Pure 100BA + 50µl ct capped Au nanoparticle dispersion

**b) Estimation of order parameter S from Birefringence  $\delta n$ :**

A simple procedure is proposed for the determination order parameter S from the birefringence measurements  $\delta n$  without considering the local field experienced by the molecule in a liquid crystal phase<sup>19</sup>. The birefringence  $\delta n$ , which is a function of temperature is fitted to the following equation,  $\delta n = \Delta n \{1 - (T/T^*)\}^\beta$ . Where T is the absolute temperature,  $T^*$  and  $\beta$  are constants. ( $T^*$  is about 1-4K higher than the clearing temperature and the exponent  $\beta$  is close to 0.2). This procedure enables one to extrapolate  $\delta n$  to the absolute zero temperature. In practice, the three adjustable parameters  $T^*$ ,  $\Delta n$  and  $\beta$  were obtained by fitting the experimental data for  $\delta n$  to the following equation written in the logarithmic form:

$$\text{Log } \delta n = \text{log } \Delta n + \beta \text{ log } \{1 - (T/T^*)\}$$

In the present investigations, the value of  $\text{log } \Delta n$  and  $\beta$  are estimated by the linear regression and the corresponding values for 100BA and 100BA+ 50µl ct capped Au nanoparticles dispersion is shown in the Table-2. Only the nematic range is considered for the evaluation of  $\Delta n$  from this method. The order parameter S value is estimated from the equation  $S = \delta n / \Delta n$ . Where  $\Delta n$  is the birefringence anisotropy in perfect order which is obtained from the log-log plots of experimental  $\delta n$  and the reduced temperature. The

variation of order parameter LC compound pure 10OBA and 10OBA + 50 $\mu$ l ct capped Au nanoparticles dispersion with temperature is shown in Fig.16. While dispersing the Au nanoparticles in 10OBA, the order parameter is increased by 1.9%. The order parameter enhancement is of primary importance for the innovation of different electro-optic applications.

**Table-3 Parameters for the best fit through linear regression for the equation  $\text{Log } \delta n = \log \Delta n + \beta \log \{1 - (T/T^*)\}$**

Compound	$T^* = T + \dots$	Slope ( $\beta$ )	$\text{Log}(\Delta n)$	$\Delta n$	R
10OBA pure	1.7	0.2082	-0.5236	0.3	0.9959
10OBA +50 $\mu$ lct capped Au	0.5	0.2052	-0.522	0.3	0.9869

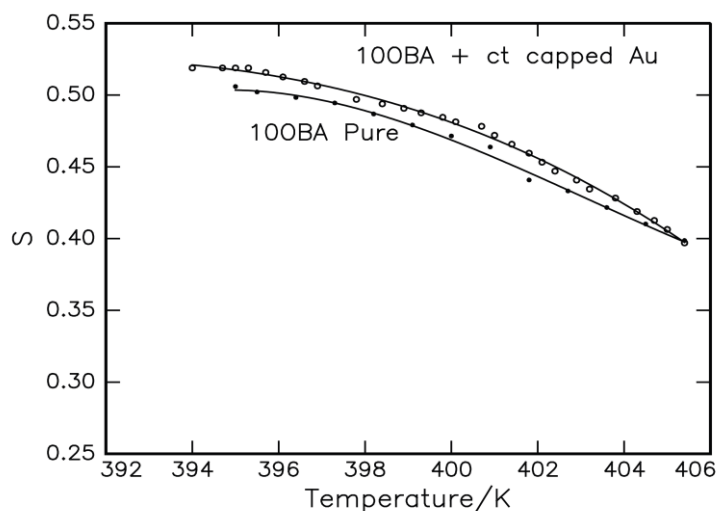


**Fig.14** Order parameter, S versus temperature for the compound 10OBA pure and 10OBA with 50  $\mu$ l ct capped Au nanoparticles

### Conclusion:

With the present results we demonstrated the dispersion of ct capped Au nanoparticles in LC 10OBA and 11OBA changing of their textures, phase transition temperatures by using Polarizing Microscope and Fourier Transform Infra Red techniques respectively. The presence of ct capped Au nanoparticles in 10OBA is also confirmed by the EDS data of SEM and UV spectrometry. X-Ray diffraction confirms that no alteration of its structure and also the existence of the ct capped Au nanoparticles and from Scherrer's Formula, the size of the citrate capped nanoparticles is found to be 29nm. It is further found that the orientational order parameter S with respect to temperature is increased by 2% nearly with the dispersion of ct capped Au nanoparticles.

### Acknowledgements:

The author Dr R.K.N.R. Manepalli (Dr M. Ramakrishna NancharaRao) is thankful to UGC for grant 42-784/2013 (SR).

### References:

1. Kato, T., Mizoshita, N. and Kishimoto, K. (2006). Functional liquid crystalline assemblies: Self organized soft materials. *Angew, Chem., Int. Ed.*, 45: 38-68.
2. Goodby, J.W., Saez, I.M., Cowling, S.J., Gortz, V., Drapper, M., Hall, A.W., Sia, S., Cosquer, G., Lee, S.E. and Raynes, E.P. (2008). Nanostructured liquid crystals *Angew. Chem. Int. E.*, 47: 2754-2787.

3. Tschiersle, C. (2007). The application of heat transfer fluids. *Chem. Soc. Rev.*, 36: 1930-1970.
4. Narayanan, R. and El-Sayed, M.A. (2005). Structure and Functional Properties Colloidal Systems. *J. Phys. Chem. B.*, 109: 12663-12676.
5. Elghanian, R., Storhoff, J.J., Mucic, R.C., Letsinger, R.L. and Mirkin, C.A. (1997). Nano Surface Chemistry. *Science*, 277: 1078-1081.
6. Brust, M. and Kiely, C. (2002). Green synthesis of silver nanoparticles using negatively charged heparin. *Surf. A: Physicochem. Engg. Aspects*, 202(2-3): 175-186.
7. Giersig, M. and Mulvaney, P. (1993). Handbook of Nanostructured Materials and Nanotechnology. *J. Phys. Chem.*, 97: 6334-6336.
8. Storhoff, J.J. and Mirkin, C.A. (1999). Self-assembly of mesogens-decorated gold nanoparticles. *Chem. Rev.*, 99: 1849-1857.
9. Rao, M.C. and Ramachandra Rao, K. (2014). Thermal Evaporated V<sub>2</sub>O<sub>5</sub> Thin Films: Thermodynamic Properties. *Int. J. Chem Tech Res.*, 6(7): 3931-3934.
10. Rao, M.C. (2014). Vacuum Evaporated V<sub>2</sub>O<sub>5</sub> Thin Films for Gas Sensing Application. *Int. J. Chem Tech Res.*, 6(3): 1904-1906.
11. Prasad, P.V., Ramachandra Rao, K., Rao, M.C. (2014). Spectroscopic Studies on Pure and Mn<sup>2+</sup> Doped Nonlinear L-Cysteine Hydrochloride Monohydrate for Electro-optic Modulation. *Int. J. Chem Tech Res.*, 7(1): 269-274.
12. Srinivasa Rao, Ch., Rao, M.C. and Srikumar T. (2014). Optical Absorption Studies on Lithium Aluminosilicate Glasses Doped with Low Concentrations of WO<sub>3</sub>. *Int. J. ChemTech Res.*, 6(7): 3935-3938.
13. Srikumar, T., Srinivasa Rao, Ch. and Rao, M.C. (2014). Physical and Optical Absorption Studies of LiF/NaF/KF-P<sub>2</sub>O<sub>5</sub>- B<sub>2</sub>O<sub>3</sub> Glasses Doped with Nd<sub>2</sub>O<sub>3</sub>. *Int. J. Chem Tech Res.*, 6(11): 4697-4701.
14. Srinivasa Rao, Ch. and Rao, M.C. (2015). Spectroscopic Studies on Alumino Alkali Zirconia Silicate Glasses Mixed with Titanium ions for Optoelectronic Device Application. *Int. J. Chem Tech Res.*, 8(2): 524-527.
15. Gray, G.W. (1962). Molecular structures and properties of liquid crystals. Academic Press.
16. Aissou, K., Fleury, G., Pecastaings, G., Alnasser, T., Mornet, S., Goglio, G. and Hadzi-ioannou, G. (2011). Hexagonal-to-cubic phase transformation in composite thin films induced by FePt nanoparticles located at PS/PEO interfaces. *Langmuir*, 27: 14481-14488.
17. Ramakrishna Nanchara Rao, M., Datta Prasad, P.V. and Pisipati, V.G. K.M. (2010). Orientational Order Parameter in Alkoxy Benzoic Acids—Optical Studies. *Mol. Cryst. Liq. Cryst.*, 528: 49-63.
18. Wu, S.T. (1986). Birefringence dispersions of liquid crystals. *Phys. Rev. A*, 33: 1270-1274.
19. Wu, S.T., Hsu, C.S. and Shyu, K.F. (1999). High birefringence and wide nematic range bis-tolane liquid crystals. *Appl. Phys. Lett.*, 74: 344-346.

\*\*\*\*\*